

Direct versus Mediated Through-Space Magnetic Interactions: A First Principles, Bottom-Up Reinvestigation of the Magnetism of the Pyridyl-Verdazyl:Hydroquinone Molecular Co-Crystal

Joaquim Jornet,^[a] Mercè Deumal,^{*[a]} Jordi Ribas-Ariño,^[a] Michael J. Bearpark,^[b] Michael A. Robb,^[b] Robin G. Hicks,^[c] and Juan J. Novoa^{*[a]}

Abstract: The mechanism of the magnetic interaction in the pyridyl-verdazyl radical:hydroquinone (pyvd:hq) molecular co-crystal is important as it has been suggested to originate by a unique “mediated through-space” magnetic interaction. This interaction was proposed to magnetically connect two nonadjacent pyridyl-verdazyl radicals within a π stack, where adjacent radicals pile up in a head-over-tail orientation. The connection is made through a third radical sitting between the previous two mediated radicals. Given the relevance of this proposal, we decided to reinvestigate the magnetic properties of this co-crystal by using our recently proposed first-principles “bottom-up” procedure. Based on B3LYP/6-31+G(d) and CASSCF(6,6)/6-31+G(d) calculations (the results of which are identical to those provided by CASSCF(10,10)/6-31+G(d) calcula-

tions), we have computed the microscopic J_{AB} values for all direct through-space magnetic interactions between nearby pyridyl-verdazyl radicals. The magnetic interactions give rise to two dominant values of similar strength: -56 and -54 cm^{-1} at the B3LYP level, which are calculated as -38 and -31 cm^{-1} at the CASSCF(6,6) and CAS(10,10) levels (all other interactions being smaller than $|1|$ cm^{-1}). The dominant interactions correspond to the direct through-space interaction between two adjacent radicals of a π stack. The crystal also exhibits a radical-mediated through-space interaction of -0.31 cm^{-1} between two nonadja-


cent radicals of a π stack. The direct through-space magnetic interactions are two orders of magnitude larger than the mediated through-space interaction. Thus, first-principles calculations do not support a mediated through-space mechanism to explain the magnetism of the pyvd:hq co-crystal. The magnetic topology generated by the two dominant antiferromagnetic interactions in the pyvd:hq co-crystal consists of one-dimensional (1D) alternating chains (interacting very weakly along the b and c axes). By using this topology, the computed macroscopic magnetic susceptibility curve reproduces the experimental one properly. This first-principles bottom-up description of the magnetism in the pyvd:hq co-crystal differs in some fundamental aspects from that previously proposed in the literature.

Keywords: density functional calculations • magnetic properties • radicals • through-bond interactions • through-space interactions

[a] J. Jornet, Dr. M. Deumal, J. Ribas-Ariño, Prof. J. J. Novoa
Departament de Química Física
Facultat de Química, Universitat de Barcelona
and CERQT, Parc Científic, Universitat de Barcelona Martí i Franquès
1, 08028-Barcelona (Spain)
Fax: (+34)93-402-1231
E-mail: m.deumal@qf.uf.es
juan.novoa@ub.edu

[b] Dr. M. J. Bearpark, Prof. M. A. Robb
Chemistry Department, Imperial College London
South Kensington Campus, SW7 2AZ, London (UK)

[c] Dr. R. G. Hicks
Department of Chemistry, University of Victoria
BC (Canada)

 Supporting information for this article is available on the WWW under <http://www.chemeurj.org/> or from the authors. Comparison between experimental and calculated $\chi(T)$ values; information on extended models to study the convergence of the magnetic susceptibility versus temperature; effect on the calculated $\chi(T)$ values of including the $J_{\text{ms}}^{\text{hq}}(dII)$ contribution along the b axis; effect on the calculated $\chi(T)$ values of accounting for the radical-mediated through-space $J_{\text{ms}}^{\text{rad}}(d8)$ (-0.31 cm^{-1}) magnetic interactions.

Introduction

Purely organic molecular magnets are a class of intensely investigated molecule-based magnets.^[1] Progress in the field has been difficult due to the lack of a full understanding of the factors that govern the mechanism according to which the magnetic interactions propagate within a molecular magnet. This gives rise to the absence of properly based magneto-structural correlations (e.g., the McConnell-I^[2a] and -II^[2b] mechanisms have been shown to fail in many

cases and lack a proper theoretical foundation)^[2c,d]. Therefore, any new data that provides relevant information about the mechanism of the magnetic interaction in these systems is of interest to design new materials that hopefully show improved magnetic properties.

It is commonly assumed that magnetism in these purely organic molecular magnets results from the through-space interaction of nearby radicals, the origin of which can be attributed to the direct overlap of the orbitals of these radicals. Throughout this work, this mechanism will be referred

Abstract in Catalan: *El mecanisme de la interacció magnètica en el co-cristall molecular de piridil-verdazil:hidroquinona (pyvd:hq) és important ja que s'ha suggerit que el seu origen és degut únicament a una interacció magnètica assistida a través de l'espai (mediated through-space). Aquesta interacció s'encarregaria de connectar magnèticament dos radicals de piridil-verdazil no adjacents dins d'un apilament π , on radicals adjacents s'apilen en una orientació antiparal·lela (head-over-tail). La connexió té lloc via un tercer radical, situat entre els dos radicals anteriors, que els assisteix. Donada la novetat i la possible rellevància de la proposta, s'ha decidit reinvestigar les propietats magnètiques d'aquest co-cristall usant un procediment bottom-up de primers principis que ha estat recentment proposat. El valor de les J_{AB} microscòpiques de totes les interaccions directes a través de l'espai entre radicals piridil-verdazil veïns s'ha calculat a nivell B3LYP/6-31+G(d) i CASSCF(6,6)/6-31+G(d). Aquestes interaccions magnètiques presenten dos valors dominants de magnitud similar: -56 i -54 cm^{-1} a nivell B3LYP, que es converteixen en -38 i -31 cm^{-1} a nivell CASSCF(6,6) i CASSCF(10,10) (la resta d'interaccions tenen valors més petits que $|1|$ cm^{-1}). Les dues interaccions dominants corresponen a interaccions directes a través de l'espai entre dos radicals adjacents d'un apilament π . El cristall també presenta una altra interacció a través de l'espai entre dos radicals no adjacents d'un apilament π , assistida per un tercer radical, de 0.31 cm^{-1} . Les interaccions magnètiques directes a través de l'espai són dos ordres de magnitud més grans que la interacció assistida a través de l'espai. Així doncs, els càlculs basats en primers principis no recolzen el mecanisme assistit a través de l'espai per explicar el magnetisme del co-cristall de pyvd:hq. La topologia magnètica generada amb les dues interaccions antiferromagnètiques dominants en el co-cristall de pyvd:hq consisteix en cadenes 1D alternades, que interaccionen molt dèbilment al llarg dels eixos b i c. D'acord amb aquesta topologia, la corba calculada de la susceptibilitat magnètica macroscòpica reproduïx correctament l'experimental. La descripció del magnetisme en el co-cristall de pyvd:hq usant un mètode basat en càlculs de primers principis bottom-up difereix, doncs, en alguns aspectes fonamentals de la proposada en la literatura anteriorment.*

Abstract in Spanish: *El mecanismo de la interacción magnética en el co-cristal molecular de piridil-verdazil:hidroquinona (pyvd:hq) es importante ya que se ha sugerido que su origen se debe únicamente a una interacción magnética asistida a través del espacio. Esta interacción se encargaría de conectar magnéticamente dos radicales de piridil-verdazil no adyacentes de un mismo apilamiento π , dentro del cual radicales adyacentes se apilan siguiendo una orientación antiparalela (cabeza-sobre-cola). La conexión tiene lugar via un tercer radical, situado entre los dos radicales anteriores, que actúa de asistente. Dada la novedad de este mecanismo y su posible relevancia, se ha decidido reinvestigar las propiedades magnéticas de este co-cristal usando un procedimiento bottom-up de primeros principios, recientemente propuesto. El valor de las J_{AB} microscópicas de todas las interacciones directas a través del espacio entre radicales piridil-verdazil vecinos se ha calculado a nivel B3LYP/6-31+G(d) y CASSCF(6,6)/6-31+G(d) (método que proporciona resultados similares al de cálculos CASSCF(10,10)/6-31+G(d)). Estas interacciones magnéticas presentan dos valores dominantes de magnitud similar: -56 y -54 cm^{-1} a nivel B3LYP, que se convierten en -38 y -31 cm^{-1} a nivel CASSCF(6,6) y CASSCF(10,10) (las demás interacciones tienen valores inferiores a $|1|$ cm^{-1}). Las dos interacciones dominantes se corresponden a interacciones a través del espacio directas entre radicales contiguos de un mismo apilamiento π . El cristal también presenta otra interacción a través del espacio asistida por un tercer radical, entre dos radicales no contiguos de un mismo apilamiento π , cuyo valor es 0.31 cm^{-1} . Luego, las interacciones magnéticas a través del espacio directas son dos ordenes de magnitud más grandes que la interacción a través del espacio asistida. En resumen, cálculos basados en primeros principios no justifican el usar el mecanismo asistido a través del espacio para explicar el magnetismo del co-cristal de pyvd:hq. La topología magnética generada por las dos interacciones antiferromagnéticas dominantes en el co-cristal de pyvd:hq consiste en cadenas 1D alternadas, que interaccionan muy débilmente a lo largo de los ejes b y c. La curva calculada a partir de esta topología para la susceptibilidad magnética macroscópica reproduce correctamente la curva experimental. Por lo tanto, la descripción del magnetismo en el co-cristal de pyvd:hq obtenida usando un método basado en cálculos de primeros principios bottom-up, difiere en aspectos fundamentales de la propuesta anteriormente en la literatura.*

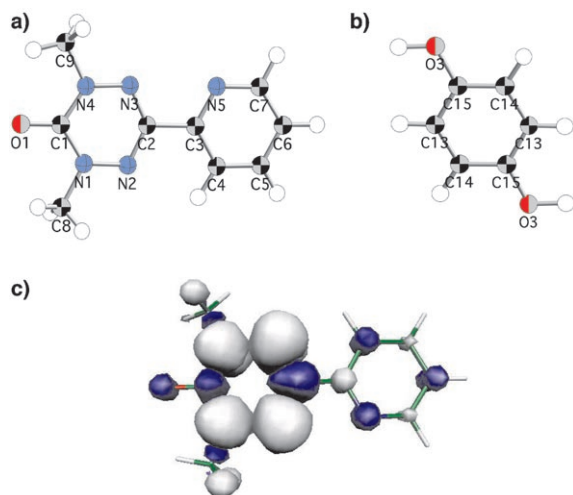


Figure 1. Chemical formula of the pyridyl-verdazyl radical (a), and the hydroquinone molecule (b), as well as the calculated spin density of the pyridyl-verdazyl radical (c). Light shading indicates positive spin density, and dark shading indicates negative spin density (isodensity surface of 0.001 au). Notice that although there is π spin density distribution on both pyridyl and verdazyl rings, the main contribution is located on the NNC_2NN fragment of the verdazyl group.

to as the “direct through-space” mechanism. However, in a recent study on the magnetism of the pyridyl-verdazyl:hydroquinone (pyvd:hq) molecular co-crystal^[3] (see Figure 1 for chemical formula and spin distribution), the authors proposed a new through-space mechanism of magnetic interaction, where the orbitals of the radicals interact due to the mediating action of another molecule (either a diamagnetic molecule or the diamagnetic part of a radical^[3]). This mechanism closely resembles the metal...ligand...metal superexchange through-bond interactions, where two spin-containing metals are connected by means of the orbitals of a diamagnetic ligand. Therefore, it will be referred to as the “mediated through-space” mechanism.

The reason to suggest a mediated through-space mechanism is connected to the crystal packing of the spin-containing units in the pyvd:hq molecular co-crystal. The pyridyl-verdazyl radicals pile up in stacks (identified later on as π stacks) along the a axis. Within these π stacks, adjacent radicals pack parallel to each other in a head-over-tail (verdazyl ring over pyridyl ring) disposition. As a consequence, the verdazyl ring of one radical is nearly perfectly aligned to the pyridyl ring of its nearest neighbor within the stack (the shortest distances being 3.415 and 3.523 Å, see Figure 2a). In such a disposition, the spin-containing regions of the radicals (the verdazyl ring) cannot present short contacts between adjacent radicals. Therefore, the authors^[3] (biased by the McConnell-I mechanism^[2a]) assumed that no magnetic interactions between adjacent radicals of the same π stack could exist, although such a hypothesis was not supported by numerical calculations. According to such a hypothesis, given the packing of the pyvd:hq crystal (Figure 2), no magnetic interaction should exist among the radicals in this crystal, a fact that contradicts the experimentally observed anti-

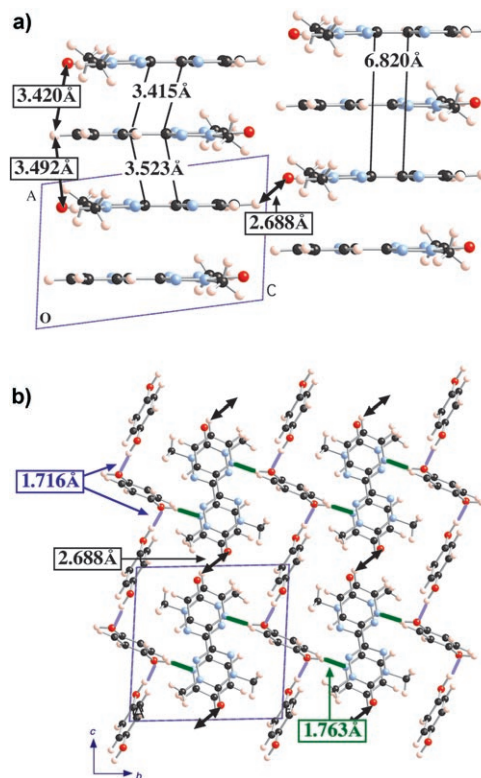


Figure 2. a) Head-over-tail (verdazyl-over-pyridyl) and head-over-head (verdazyl-over-verdazyl) π stacking of pyridyl-verdazyl radicals along the a axis, with 3.415/3.523 and 6.820 Å being the shortest inter-radical distances within a π stack, respectively. Shortest C-H...O hydrogen bonds are also indicated. b) Molecular packing of pyridyl-verdazyl radicals and hydroquinone molecules within a bc layer. Notice the two-dimensional (bc plane) net of hydrogen bonds is explicitly shown as lines connecting either two hydroquinone molecules or two pyridyl-verdazyl radicals along the c axis (at 1.716 and 2.688 Å, respectively) or a hydroquinone molecule and a pyridyl-verdazyl radical along the b axis (at 1.763 Å).

ferromagnetic interactions. Therefore, based on BP86/DZVP density functional calculations,^[3] the authors proposed that antiferromagnetic interactions could exist in trimers of pyridyl-verdazyl radicals, their existence being attributed to the mediating action of the diamagnetic pyridyl ring of the middle radical (see verdazyl...verdazyl distance of 6.82 Å in Figure 2a). The experimental magnetic susceptibility $\chi(T)$ curve was thus fitted to a 1D regular chain model.^[4,5] Each π stack of radicals was suggested to contain two such chains that could give rise to a molecular spin-ladder magnetic topology, if a weak interaction between them were to exist.^[3]

Given the interest and relevance of that proposal referring to through-space magnetism, we decided to perform a detailed reinvestigation of the role of the direct and mediated through-space magnetic interactions in the pyvd:hq molecular co-crystal. Such analysis will be part of a full first-principles bottom-up study of the magnetic properties of this crystal. Such a procedure was designed to allow a systematic and unbiased study of the magnetic properties of a crystal avoiding any assumptions on the nature of its mag-

netic interactions. The procedure systematically evaluates the ferro- or antiferromagnetic nature of all unique microscopic J_{AB} magnetic interactions present in the crystal at the B3LYP level. The B3LYP results are also supported by CASSCF(6,6) and CASSCF(10,10) calculations. Then, the magnetic topology of the magnetic interactions within the crystal can be defined in terms of all non-negligible J_{AB} parameters and their connectivity. The macroscopic magnetic properties (e.g., the magnetic susceptibility (χ) or the shape of the χT versus T curve) are finally computed by using an accurate numerical procedure, and are compared to the available experimental data. This first-principles bottom-up procedure has been previously shown to reproduce the known experimental magnetic properties (magnetic susceptibility curves, heat capacity, spin-gap and so forth) of a variety of purely organic and metal-containing molecular crystals.^[6–8]

The application of our first-principles bottom-up procedure to study the magnetic properties of the pyvd:hq co-crystal provided some surprising findings when we compared our results with those reported in the literature.^[3] First of all, our results do not support the mediated through-space mechanism as being responsible for the magnetism of the pyvd:hq co-crystal. Instead, the magnetism is due to two direct through-space interactions between adjacent radicals of the same π stack. However, such mediated through-space magnetic interactions should be taken into account in cases where there are no direct through-space interactions. Secondly, no molecular spin-ladder magnetic topology is supported by our first-principles calculations. The magnetic topology defined by the two dominant magnetic interactions consists of 1D alternating chains (interacting very weakly along the b and c axes). Finally, by using this topology, the computed macroscopic magnetic susceptibility curve accurately reproduces the experimental one above 20 K (below this temperature, the presence of impurities masks the measured $\chi(T)$ values).

Computational Details

The main steps and underlying physics behind the first-principles bottom-up procedure that we used to study the magnetic properties of the pyvd:hq molecular co-crystal are briefly described below. A detailed mathematical and physical account of the procedure and its foundations can be found in the literature.^[6]

The basic idea behind our bottom-up procedure was to find a finite model space that accurately describes the properties of the magnetic topology of the crystal. This space was used to compute the matrix representation of the Heisenberg Hamiltonian [Eq. (1)], in which \hat{S}_A and \hat{S}_B are the spin operators associated with radicals A and B, and \hat{I}_{AB} the identity operator.

$$\hat{H} = - \sum_{A,B}^N J_{AB} (2\hat{S}_A \cdot \hat{S}_B + 1/2\hat{I}_{AB}) \quad (1)$$

The only variables in this Hamiltonian are the microscopic J_{AB} parameters defining the nature and size of the radical–radical magnetic interactions present in our model space. It is worth mentioning here that the

Heisenberg Hamiltonian of Equation (1) and the more usual $\hat{H}_{AB} = -2\sum J_{AB}\hat{S}_A \cdot \hat{S}_B$ have the same energy differences between spin states, since their energy spectra only differ by a shift in all individual energy values. Consequently, both Hamiltonians provide the same computed macroscopic properties.^[9] We use the Heisenberg Hamiltonian from Equation (1) for compatibility with our computer programs. Also note that the microscopic J_{AB} parameters in Equation (1) depend on the relative orientation of the A,B radicals. They can be computed by using the appropriate quantum-chemical methods (in our case, the B3LYP density functional first-principles method and the CASSCF(6,6) or CASSCF(10,10) ab initio methods).

The values of the J_{AB} parameters are also used to define the magnetic topology of the crystal under study. Such topology is defined in terms of the connectivity that the J_{AB} magnetic-pair interactions establish between the radicals constituting the crystal. The magnetic topology gives a very useful pictorial representation of the magnetic pathways within the crystal, and is very helpful to choose the finite space used to compute the Heisenberg Hamiltonian matrix associated to Equation (1).

We found that the following four steps allowed us to carry out the above-proposed first-principles bottom-up procedure in an unbiased form:

- 1) The first step consisted of a detailed analysis of the crystal packing to identify all unique A–B radical–radical pairs whose inter-pair distance was smaller than a given threshold value (above which the magnetic interaction between radicals was expected to be negligible). This threshold was deliberately chosen to select more pairs than the first nearest-neighbors (the usual candidates in the literature). Such a selection procedure of radical–radical pairs was therefore completely nonbiased.
- 2) For all A–B radical–radical pairs selected in step (1), we obtained the value of the corresponding J_{AB} magnetic-pair interaction by using quantum-chemical methods.
- 3) By using the computed J_{AB} magnetic-pair-interaction values, we then defined the magnetic topology of the crystal in terms of how non-negligible J_{AB} interactions propagated along the crystal axes. Two neighboring A–B radical sites are connected whenever their magnetic interaction presents a $|J_{AB}|$ value larger than a given threshold that in previous calculations was estimated to be $|0.05| \text{ cm}^{-1}$. Then, we searched for the smallest (finite-sized) minimal magnetic model space that describes the magnetic interactions of the whole crystal in a balanced way. The repetition of such a minimal model along the a,b,c crystallographic directions should regenerate the magnetic topology of the whole crystal. The radical centers constituting the minimal magnetic model defined a spin space that was used to compute the matrix representation of the Heisenberg Hamiltonian [Eq. (1)]. Notice that the only parameters required to compute that matrix representation of the Heisenberg Hamiltonian are the J_{AB} parameters computed in step (2).
- 4) In the last step, the Heisenberg Hamiltonian matrix was diagonalized to obtain the energy for all possible spin states. These energies were then used to compute the magnetic susceptibility $\chi(T)$ and/or heat capacity $C_p(T)$ by using adequate expressions obtained from a statistical mechanics treatment.^[6,9]

The minimal magnetic model space must be small enough to keep the Heisenberg Hamiltonian matrix at a reasonable size (in our current implementation $N \leq 16$ spin-radical sites), but it must also be large enough to contain all significant magnetic pathways detected within the crystal. From our experience, the most important step in the above procedure was the selection of a proper minimal magnetic model space. To validate the selected minimal magnetic model space, we checked the convergence of macroscopic properties (e.g., $\chi(T)$) as the model space is replicated along the three crystallographic directions applying a regionally reduced density matrix approach: if the minimal magnetic model space is properly chosen, the computed $\chi(T)$ values by using such extended models should rapidly converge to the values obtained with the nonreplicated minimal model space. All sets of results should also numerically reproduce the experimental $\chi(T)$ data.

As indicated above, the values of the microscopic J_{AB} pair interactions were computed by using quantum-chemical methods. In the pyvd:hq molecular co-crystal, the pyridyl-verdazyl radicals are the only spin-contain-

ing units. The role of the electronically closed-shell hydroquinone molecules is to stabilize the crystal packing by means of two types of hydrogen bonds established between: 1) hydroxy groups from two different hydroquinones along the *c* axis (at 1.716 Å) and, 2) the nitrogen atom of the pyridyl ring of a radical and the hydroxy group from a hydroquinone molecule along the *b* axis (at 1.763 Å) (see Figure 2b for a *bc* view). The ground electronic state of the pyridyl-verdazyl radicals is a doublet, with the spin mostly distributed on the verdazyl ring (Figure 1c and Table 1).

Table 1. Unrestricted DFT-calculated spin population for pyridyl-verdazyl radical (pyvd). The atom numbering is as in Figure 1a.

Atom verdazyl	Spin population	
	UB3LYP	UBP86 (original paper ref. [3])
O1	-0.011	-0.011
N1	0.189	0.198
N2	0.402	0.343
N3	0.403	0.342
N4	0.199	0.204
C1	-0.039	-0.016
C2	-0.167	-0.067
C8	-0.011	-0.006
C9	-0.015	-0.008
pyridyl		
N5	-0.020	-0.011
C3	0.025	0.008
C4	-0.010	-0.010
C5	0.022	0.008
C6	-0.024	-0.011
C7	0.012	0.007

As the radicals are doublets, the value of J_{AB} for each radical-radical pair is obtained by subtracting the energy of the most stable open-shell singlet and the triplet states. The open-shell singlet can only be properly described at the density functional level^[10] by using the broken-symmetry approximation.^[11] Thus, keeping in mind that in computations we used the Heisenberg Hamiltonian [Eq. (1)], equivalent to the most usual form $\hat{H}_{AB} = -2\Sigma J_{AB}\hat{S}_A\cdot\hat{S}_B$, the J_{AB} parameters in our B3LYP calculations were computed as given in Equation (2), in which E_{BS}^S and E^T correspond to the energy of the lowest energy broken-symmetry singlet and triplet states, both computed at the geometry of the radical-radical pair found in the crystal.

$$E_{BS}^S - E^T = J_{AB} \quad (2)$$

In both cases, we used the unrestricted formulation of the density functional equations^[12] (a 10^{-8} convergence criterion on the total energy and 10^{-10} on the integrals was used to ensure enough accuracy in the computation of the J_{AB} parameters), and the basis set was a 6-31+G(d)^[13] for all atoms. In our CASSCF(6,6) calculations, the J_{AB} parameters were obtained by selecting the lowest energy singlet and triplet states provided by a MCSCF calculation with a complete active space containing six electrons in six orbitals. An equivalent procedure was used in our CASSCF-(10,10) calculations (it is worth noting here that the occupations of the fourteen natural orbitals closer to the SOMO obtained for the triplet in a UB3LYP calculation are: 1.94, 1.93, 1.89, 1.89, 1.81, 1.79, 1.00, 1.00, 0.21, 0.19, 0.11, 0.11, 0.07, and 0.06 atomic units, numbers that explain our choice of active spaces in the CASSCF calculations). All DFT and CASSCF calculations performed in this study were carried out with the Gaussian 03 and GAMESS packages,^[14] respectively.

Results and Discussion

The pyridyl-verdazyl radical co-crystallizes with hydroquinone diamagnetic molecules (see Figure 2 for crystal pack-

ing). This crystal belongs to the $P\bar{1}$ space group (triclinic), with cell parameters (at 298 K) being $a=6.820$, $b=10.450$, and $c=10.738$ Å, $\alpha=85.930$, $\beta=80.161$, and $\gamma=87.029^\circ$.^[3] Within each pyridyl-verdazyl radical, the pyridyl and verdazyl six-membered rings are almost planar and nearly coplanar to each other (torsion angle = 2.4°).

As mentioned before, the packing structure of this co-crystal is characterized by the presence of π stacks of pyridyl-verdazyl radicals piled up along the *a* axis in a head-over-tail (that is, verdazyl ring over pyridyl ring) arrangement (see Figure 2a, where the inset shows possible C-H...O hydrogen bonds at 3.420 and 3.492 Å). Along the *c* axis (see Figure 2a), π stacks are connected to other π stacks by C-H...O hydrogen bonds at 2.688 Å, forming *ac* planes. Along the *b* axis (see Figure 2b), two *ac* planes of π stacks are separated by planes of hydroquinone molecules that are held together by C-H...O hydrogen bonds between two hydroquinones at 1.716 Å. Finally, hydroquinone molecules and pyridyl-verdazyl radicals also establish C-H...O hydrogen bonds at 1.763 Å (Figure 2b).

The magnetic properties of the pyvd:hq co-crystal originate at the pyridyl-verdazyl radical. The spin density (Figure 1c and Table 1) is distributed on both pyridyl and verdazyl rings, although the main contribution is located on the verdazyl ring (more specifically on the π system of the NNC₂NN fragment, see Figure 1). The four N atoms on the verdazyl ring have positive spin density and the C2 atom carries a negative spin density.^[15] The crystal packing (Figure 2) does not allow the existence of short contacts between the high-spin regions of the pyridyl-verdazyl radicals. According to the McConnell-I mechanism,^[2a] no magnetic interactions should thus exist between adjacent radicals in these π stacks, and also between stacks. Therefore, the crystal should behave as a paramagnet.

In contrast to what we expect from the McConnell-I model, the experimental magnetic properties indicate the presence of antiferromagnetic interactions.^[3] The experimental magnetic susceptibility curve was fitted to a 1D regular chain model, based on the Heisenberg Hamiltonian $\hat{H}_{\text{fitting}} = -\Sigma J_{\text{fit}}\hat{S}_A\cdot\hat{S}_B$ (notice that, in the original paper,^[3] there was an erratum concerning the J_{fit} value, as we later found from numerical simulations by using the fitting expression from reference [4], see Supporting Information Figure S1). The parameters that provided the least-squares best-fit were $J_{\text{fit}} = -116$ cm⁻¹, $\theta = -3$ K, $g = 2.0025$.^[3,4] We must stress here that J_{fit} cannot be ascribed to any individual radical-radical J_{AB} magnetic interaction, but averages all of them. Notice that in our computations (e.g., energies, magnetic susceptibility, and so on), the Heisenberg Hamiltonian is expressed as in Equation (1), equivalent to $\hat{H}_{AB} = -2\Sigma J_{AB}\hat{S}_A\cdot\hat{S}_B$, that differs from the fitting Hamiltonian by a factor of two. Therefore, to compare any computed J_{AB} value to J_{fit} , one should compare our computed J_{AB} values to $J_{\text{fit}}/2 = -58$ cm⁻¹.

Hereafter, we present the results of our study in four sections, one for each of the steps involved in the first-principles bottom-up procedure.

Step 1: identification of all unique radical–radical pairs within the crystal: We first analyzed the crystal packing (Figure 2) looking for all unique radical–radical pairs (hereafter identified as d_i) that could generate magnetic interactions. As any direct through-space magnetic interaction is a consequence of the direct overlap of the orbitals of the interacting radicals, it decreases exponentially as the distance between the radical centers increases. We therefore selected all radical–radical pairs with inter-radical distances shorter than 7.0 Å. Such a cut-off value was large enough to include all first-nearest neighbors around a given radical ($d1$ – $d5$ in Figure 3, see Table 2 for inter-radical distances) and the most relevant second-nearest neighbors ($d6$ – $d9$ in Figure 3) (notice that the lines between radicals in Figure 3 do not represent bonds but potential magnetic interactions, and that the atoms connected are those with the shortest inter-radical distance in Table 2). The nine $d1$ – $d9$ radical–radical candidates are distributed forming a plane of π stacks, along the a and c axes (Figure 3a). Three pairs ($d2$, $d4$, and $d8$) correspond to possible interactions within the same π stack of radicals along the a axis, and the remaining pairs ($d1$, $d3$, $d5$ – $d7$, $d9$) connect radicals that belong to two adjacent π stacks.

To allow a numerical evaluation of the interaction between consecutive ac planes, and despite the fact that the inter-radical distance is larger than the 7.0 Å cut-off value, we included two additional dimers ($d10$ and $d11$, shown in Figure 3b). Radical pair $d10$ is the radical–radical pair showing the shortest inter- ac -plane intermolecular distance, and was selected to study the direct interplane radical–radical magnetic interactions. Radical pair $d11$ was selected to study the possible magnetic interaction of two pyridyl-verdazyl radicals mediated by a closed-shell hydroquinone molecule.

Step 2: computation of the J_{AB} magnetic interactions: The value of the J_{AB} magnetic interaction for each radical–radical pair, $J(d_i)$, was first computed at the B3LYP/6-31+G(d) level, by using for each pair of radicals its crystal geometry. Table 2 contains the B3LYP/6-31+G(d)

value for each dimer d_i , together with the shortest distance between radicals (second column), verdazyl–verdazyl rings (third column), and C2 atoms (fourth column). Clearly, there is no simple correlation between any of these distances and the magnitude of the corresponding magnetic interaction. There are only four non-negligible radical–radical interactions: $J(d2)$, $J(d3)$, $J(d4)$, and $J_{\text{mfs}}^{\text{hq}}(d11)$,^[16] whose geometries are depicted in Figure 4. Two magnetic interactions connect two adjacent radicals of a given π stack in a head-

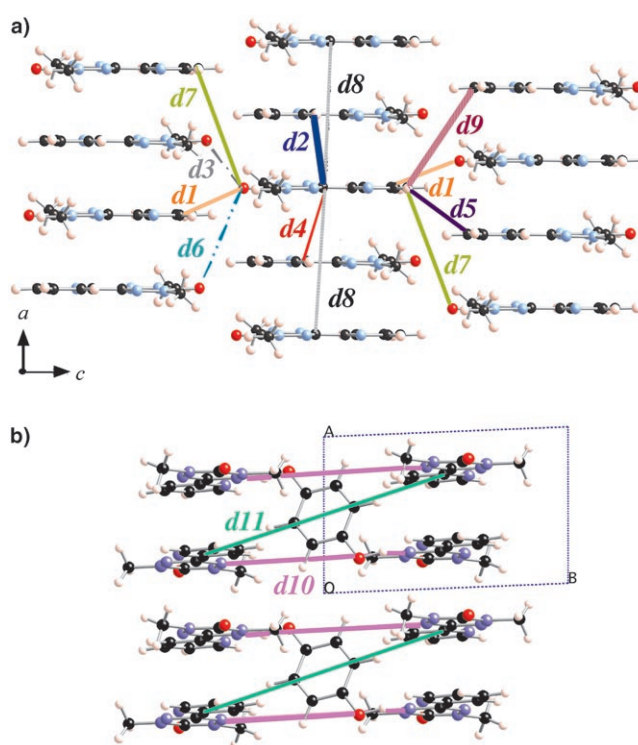


Figure 3. a) Possible pyridyl-verdazyl radical pairs d_i ($i=1$ – 9) that might interact magnetically within an ac layer. Any given radical might establish up to 12 magnetic interactions, since $d1$, $d7$, and $d8$ appear twice. b) Schematic ab view of the possible $d10$ and $d11$ pairs of radicals coupling any two-dimensional ac layers.

Table 2. Unrestricted DFT broken-symmetry UB3LYP/6-31+G(d) results for $J(d_i)$ pair interaction of all eleven candidates ($d1$ – $d11$) for the pyvd:hq crystal. Shortest distances between radicals (second column), verdazyl–verdazyl rings (third column) and C2–C2 atoms (fourth column) are given.

Dimers d_i	Shortest inter-radical contact	dist [Å]	Shortest vd–vd ring contact	dist [Å]	$d(\text{C2}–\text{C2})$ [Å]	$J(d_i)$ [cm^{-1}]
$d1$	O...C6 (vd...py)	3.354	O...C2	6.978	10.738	< 0.05
$d2$	C2...C3 (vd...py)	3.415	C2...C2, C3...C3	3.535	3.535	–54.43
$d3$	O...O (vd...vd)	3.479	O...O	3.479	9.871	+0.08
$d4$	C2...C3 (vd...py)	3.523	C2...C2, C3...C3	3.555	3.555	–55.97
$d5$	C6...C6 (py...py)	3.848	C2...C2	11.545	11.545	< 0.05
$d6$	O...O (vd...vd)	5.601	O...O	5.601	11.073	< 0.05
$d7$	O...C6 (vd...py)	6.157	O...C2	8.551	11.696	< 0.05
$d8$	C2...C2 (vd...vd)	6.820	vd...vd	6.820	6.820	< 0.05
$d9$	C6...C6 (py...py)	6.958	C2...C2	12.577	12.577	< 0.05
$d10$	N2...N3 (vd...vd)	8.107	N2...N3	8.107	10.450	< 0.05
$d11$	N2...N2 (vd...vd)	8.233	N2...N2	8.233	10.458	–0.44
	N _{py} ...O _{hq}	2.797				
	N2 _{vd} ...O _{hq}	3.121				

over-tail (verdazyl-over-pyridyl) disposition ($J(d2)$ and $J(d4) = -54.43$ and -55.97 cm^{-1} , respectively), and dominate over the remaining two $J(d_i)$, corresponding to a small ferromagnetic interaction between stacks ($J(d3) = +0.08 \text{ cm}^{-1}$) and an antiferromagnetic hydroquinone-mediated through-space interaction between two ac planes of π stacks ($J_{\text{mfs}}^{\text{hq}}(d11) = -0.44 \text{ cm}^{-1}$). Notice that the direct interaction between radicals packed in a head-over-head (verdazyl-over-verdazyl) disposition in the π stack, $J(d8)$, is smaller

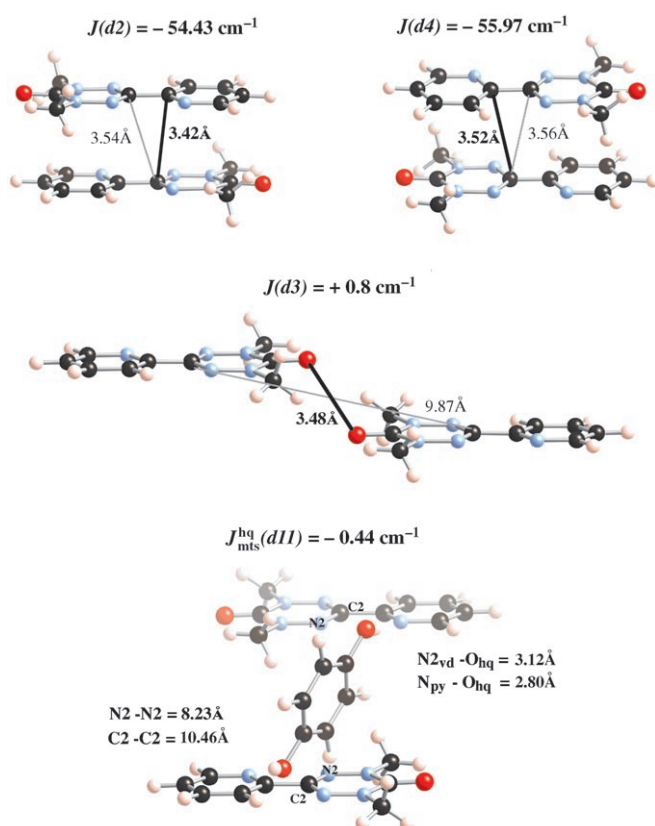


Figure 4. Geometrical disposition of numerically non-negligible $d2$, $d3$, $d4$, and $d11$ pairs of pyridyl-verdazyl radicals.

than the $|0.05| \text{ cm}^{-1}$ threshold. Therefore, our B3LYP/6-31+G(d) calculations indicate that the antiferromagnetic interactions within the pyvd:hq co-crystal are dominated by direct through-space interactions, $J(d2)$ and $J(d4)$, and there is no need to resort to mediated through-space interactions to explain the magnetism of this crystal. For completeness, we also computed the size of the mediated through-space interactions within the π stacks (hereafter, $J_{\text{mts}}^{\text{py}}(d8)$) at the B3LYP/6-31+G(d) level. Such mediated interaction was previously associated to the mediating action of the pyridyl ring that sits between two nonadjacent pyridyl-verdazyl radicals oriented in a head-over-head conformation.^[3] Therefore, consistently with such a proposal, we estimated its value by using three adjacent radicals in the π stack and by substituting the verdazyl ring of the middle radical with a hydrogen atom (we thus use a radical \cdots pyridine \cdots radical trimer). The value obtained ($J_{\text{mts}}^{\text{py}}(d8) = -0.40 \text{ cm}^{-1}$) was similar in magnitude to $J_{\text{mts}}^{\text{hq}}(d11)$ mediated through-space interactions, but two orders of magnitude smaller than $J(d2)$ and $J(d4)$ direct through-space interactions.

The B3LYP/6-31+G(d) interpretation disagrees with that reported by using a BP86 density functional and a DZVP basis-set.^[3] Therefore, we validated the quality of the computed $J(di)$ values. In a first test, we re-evaluated $J(d2)$, $J(d4)$, and $J(d8)$ at the CASSCF(6,6)/6-31+G(d) level. For the three parameters, we obtained the following values (re-

spectively): -30.5 , -38.1 , and 0.0 cm^{-1} . The value of the largest component was recomputed at the CASSCF(10,10)/6-31+G(d) level, and we obtained a value for $J(d4)$ of 37.9 cm^{-1} , thus confirming the validity of the CASSCF(6,6)/6-31+G(d) results. Therefore, CASSCF(6,6)/6-31+G(d) results confirm the strength of the $J(d2)$ and $J(d4)$ direct through-space interactions computed at the B3LYP/6-31+G(d) level (notice that the CASSCF method usually gives values smaller than those with the B3LYP level). In a second test, we evaluated the impact of computing the $J(di)$ interactions by using a trimer model, as done by other authors,^[3] instead of using radical \cdots radical pairs. We therefore tested whether there are cooperative effects among J_{AB} values not included in a radical \cdots radical pair calculation. This was done by re-evaluating the magnitude of $J(d2)$ and $J(d4)$ magnetic interactions by using three radicals. Notice that in a trimer model: 1) the mediated through-space (mts) radical \cdots radical \cdots radical interaction $J_{\text{mts}}^{\text{rad}}(d8)$ is necessarily evaluated (see Figure 5 a); 2) the radical \cdots radical \cdots radical interaction $J_{\text{mts}}^{\text{rad}}(d8)$ is different than the radical \cdots pyridine \cdots radical interaction $J_{\text{mts}}^{\text{py}}(d8)$ computed before (the former includes also the effect of the verdazyl radical fragment). The values of the three parameters present in the trimer model are computed from the energy differences between the high-spin HS quartet ($\alpha\alpha\alpha$) state and the low-spin LS dou-

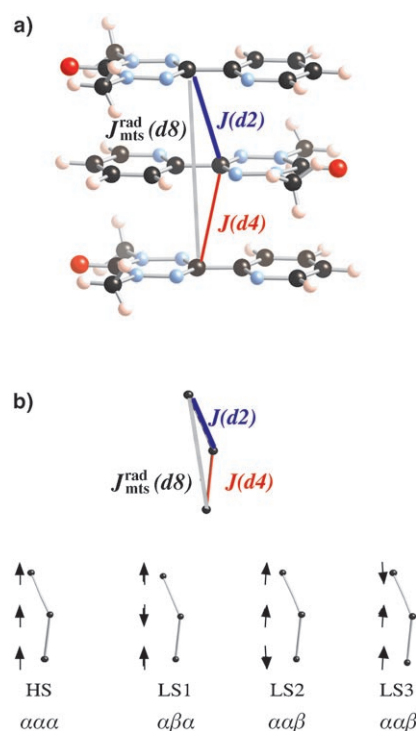


Figure 5. a) Geometrical disposition of the trimer model, where $J(di)$ radical \cdots radical interactions are shown. b) Schematic representation of three pyridyl-verdazyl radicals, where lines between atoms represent microscopic magnetic interactions instead of bonds. The solution of the corresponding secular equation problem results in a high-spin HS quartet state and three low-spin LS doublet states, namely LS1 ($\alpha\beta\alpha$), LS2 ($\beta\alpha\alpha$), and LS3 ($\alpha\alpha\beta$).

blet states ($LS1 = \alpha\beta\alpha$, $LS2 = \beta\alpha\alpha$, $LS3 = \alpha\alpha\beta$), that fulfill expressions (3)–(5)^[17] by using a broken-symmetry^[11] wavefunction (see Figure 5 b for spin states).

$$E_{HS} - E_{LS1} = -J(d2) - J(d4) \quad (3)$$

$$E_{HS} - E_{LS2} = -J(d4) - J_{\text{mfs}}^{\text{rad}}(d8) \quad (4)$$

$$E_{HS} - E_{LS3} = -J(d2) - J_{\text{mfs}}^{\text{rad}}(d8) \quad (5)$$

The following results were obtained: $J(d2) = -54.35$, $J(d4) = -55.43$, and $J_{\text{mfs}}^{\text{rad}}(d8) = -0.31 \text{ cm}^{-1}$. The values of $J(d2)$ and $J(d4)$ magnetic interactions are in very good agreement with that computed by using a radical–radical pair model (-54.43 and -55.97 cm^{-1} , Table 2). Therefore, in purely organic magnets the possible cooperative effects included by the trimer model are too small to compensate for the computational effort required to obtain the $J(di)$ value compared to its evaluation by using a radical–radical pair model. Consequently, we can conclude that our model of exchange-interaction better describes the magnetism of the pyvd:hq co-crystal. We believe that the reason is, besides any possible deficiencies associated with the BP86 functional,^[18] an oversimplistic use of expressions [Eq. (3)–(5)] to obtain the value of the magnetic interaction between nonadjacent pyridyl-verdazyl radicals (only the first expression relating the LS1 and HS states was used in the original paper^[3]).

We can now focus on the relative importance of the direct versus mediated through-space interactions. The essential point here is that the two non-negligible mediated through-space magnetic interactions computed ($J_{\text{mfs}}^{\text{rad}}(d8) = -0.31 \text{ cm}^{-1}$ and $J_{\text{mfs}}^{\text{hq}}(d11) = -0.44 \text{ cm}^{-1}$) are two orders-of-magnitude smaller than the dominant direct through-space interactions ($J(d2) = -54.43 \text{ cm}^{-1}$ and $J(d4) = -55.97 \text{ cm}^{-1}$). We have previously seen^[6–8] (and also tested in this work, see below) that the inclusion of $J_{\text{mfs}}(di)$ parameters that are much smaller than the dominant interactions has a negligible effect on the computed $\chi(T)$ curves, that is, they do not affect the macroscopic magnetic properties of the crystal. However, one should take into account these mediated through-space magnetic interactions in cases where there are no direct through-space interactions.

The magnitude of a mediated radical–ligand–radical magnetic interaction can be estimated by evaluating both the weight of the appropriate excited configurations in the trimer CASCI wavefunction (commonly known as charge-transfer configurations^[19]) and the mixing of the orbitals of the ligand and radicals. In the pyridyl-verdazyl radical, the SOMO and LUMO are centered on the verdazyl ring, and only the second LUMO is centered on the pyridyl ring. In our case, the large SOMO/second-LUMO energy difference ($\Delta E = 4.35 \text{ eV} = 35087.1 \text{ cm}^{-1}$) suggests that such mixing (if any) will be small. CASCI calculations^[14b] on the radical trimer shown in Figure 5 a by using a (3,4) active space (that includes the three unpaired electrons on each radical and four orbitals, the three SOMO orbitals and the pyridyl-cen-

tered virtual orbital of the trimer) show a negligible weight of the double-excitations (charge-transfer) from the SOMO orbitals to this virtual orbital in the antiferromagnetic state. Computations employing a larger (3,6) active space, including two extra pyridyl-centered virtual orbitals, confirm this result, that is to be expected due to the energetic inaccessibility of the double-excited configurations. Thus, one can safely conclude that the antiferromagnetic interactions in the pyvd:hq molecular co-crystal must be understood in terms of a direct through-space mechanism, involving $d2$ and $d4$ pairs of pyridyl-verdazyl radicals.

The values of $J(d2)$ and $J(d4)$ computed at the B3LYP level can now be compared with the value of J_{fit} obtained by fitting the experimental magnetic susceptibility curve by using a 1D regular-chain model,^[4] once converted to the same Hamiltonian. There is a very good agreement between $J_{\text{fit}}/2 = -58 \text{ cm}^{-1}$, and $J(d2) = -54.43$ or $J(d4) = -55.97 \text{ cm}^{-1}$. This is due to the fact that the model used in the fitting (a 1D regular chain) is very close to the magnetic topology obtained in our computational study (a nearly regular 1D chain, see below). In this model, the $J_{\text{fit}}/2$ value represents an average of the $J(d2)$ or $J(d4)$ values.

Step 3: definition of the magnetic topology and finite magnetic models: The two dominant radical–radical interactions ($J(d2)$ and $J(d4)$, see Table 2) connect the radicals of the pyvd:hq co-crystal forming an almost regular 1D chain along the a axis (within the π stacks of radicals). Adjacent 1D chains interact weakly along the b and c axes by means of $J_{\text{mfs}}^{\text{hq}}(d11)$ and $J(d3)$, respectively (Figure 6). Therefore, the magnetic topology is basically a 1D (nearly regular) alternating chain.

Once the magnetic topology has been defined, it is possible to select a set of finite models to study the convergence of the macroscopic susceptibility $\chi(T)$ data for the pyvd:hq

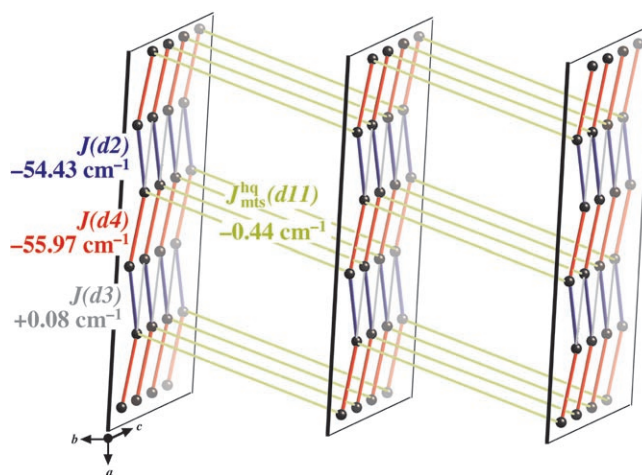


Figure 6. Schematic view of the magnetic topology of a given two-dimensional ac layer consisting of antiferromagnetic alternating $J(d2)$ and $J(d4)$ linear chains, which are weakly connected together by $J(d3)$ ferromagnetic interactions. Any two ac layers weakly interact along the b axis by means of $J_{\text{mfs}}^{\text{hq}}(d11)$ antiferromagnetic interactions.

co-crystal. All finite model spaces must be capable of reproducing the antiferromagnetic spin state with $S=0$ (absence of magnetic moment), which requires models with an even number of radical centers. Besides, the number of $J(di)$ interactions and their connectivity must reproduce all significant magnetic pathways detected within the infinite crystal in a balanced way. We will first focus on the models required to describe an isolated 1D alternating chain and, then, will address the effect of the small interchain $J(d3)$ and $J_{\text{mts}}^{\text{hq}}(d11)$ interactions.

The smallest possible chain model including $J(d2)$ and $J(d4)$ interactions and giving rise to a singlet state contains four radical sites and three radical–radical interactions (4s model in Figure 7a). However, the number of $J(d4)$ and $J(d2)$ radical–radical interactions does not give the 1:1 ratio observed in an infinite chain (it changes with the length n of the finite chain as $(n/2):(n/2)-1$, that is, for $n=4, 6, 8, 10, 12, 14$, and 16 , it takes the values 2, 1.5, 1.33, 1.25, 1.2, 1.17, and 1.14, respectively). As a consequence, in order to obtain a good accuracy in our simulations, we need alternating chain models of larger lengths than if we were to use a 1D regular chain. These alternating chain models will receive

the general name of ns models, where n is the length of the finite chain.

The study of the chain–chain interactions will be done by using $(ns+ns)$ -type models, which include two interconnected ns chains. For instance, we tested two ways of doing such an interconnection along the c axis as shown in Figure 7b, and we named them $ns+ns(1)$ and $ns+ns(2)$ models.

Step 4: computation of the magnetic susceptibility from statistical mechanics: We computed the matrix representation of the Heisenberg Hamiltonian [Eq. (1)] by using ns and $ns+ns$ finite magnetic model spaces of increasing size. From the energy spectrum, we numerically calculated the macroscopic magnetic susceptibility curves for the crystal, as shown in Figure 7.

We first analyzed the results for an isolated 1D alternating chain (Figure 7a). We used models of length ranging from $n=4$ up to 16 radical sites, and tested the convergence of the magnetic susceptibility curves $\chi(T)$ as a function of the size. We tested by comparing the results to the experimental data (Figure 7, notice that the raw experimental data (filled circles) is plotted as well as the data resulting from

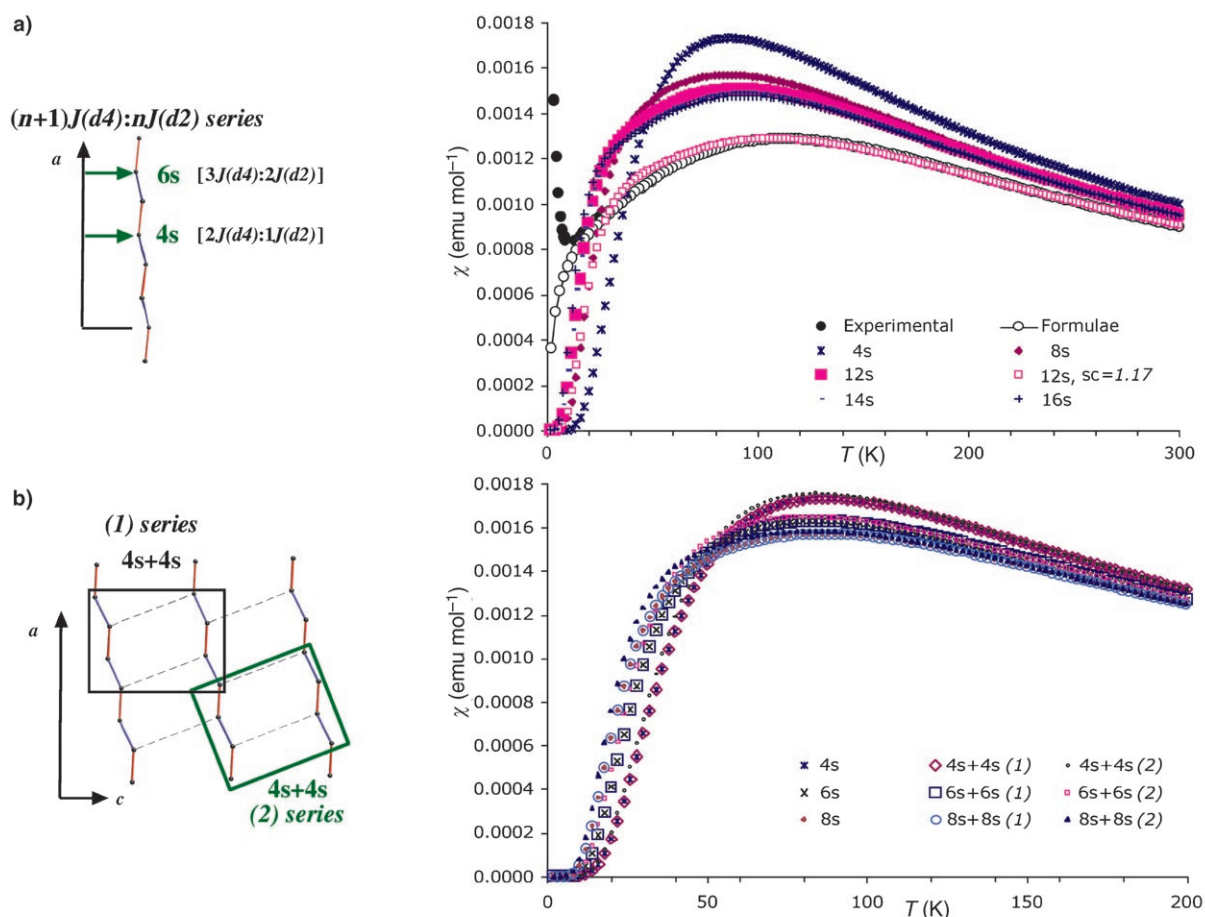


Figure 7. Computed magnetic susceptibility $\chi(T)$ values by using: a) 1D alternant chain ns models of increasing chain length from 4 to 16 (radical) spin sites along the a axis (notice that a scaling factor of 1.17 is enough in order to reproduce the experimental data with a 12-spin-site minimal model 12s); and b) Chain–chain $(ns+ns)$ models along the c axis, which do overlap with the alternating chain models.

applying the original fitting expression^[4] (empty circles)). Although none of the curves quantitatively reproduced the experimental data, a good convergence among simulated data was achieved with the model of $n=12$. This seems to indicate that a 12-spin site linear alternating chain model (12s) is the minimal magnetic model required to represent the macroscopic magnetic behavior of the pyvd:hq crystal. We fully reproduced the experimental curve after applying a small linear scaling factor of 1.17 to all energy values of the 12s minimal model. This scaling factor corrects for the use of high-temperature crystal structures instead of low-temperature ones, and for systematic errors intrinsic to our work strategy (use of the B3LYP methodology instead of full ab initio methods, possible cooperative effects, and so on). Notice we did not intend to reproduce raw experimental $\chi(T)$ data at temperatures below 20 K since the presence of impurities in the sample masks the correct experimental $\chi(T)$ values.

The effect on the $\chi(T)$ curve of including $J(d3)$ and $J_{\text{ms}}^{\text{hq}}(d11)$ interactions along the c and b axes, respectively, was tested separately by using $(ns+ns)$ -type models, where the smallest model tested interconnects two $n=4$ chains. Figure 7b shows the results obtained when $J(d3)$ was taken into account by using $ns+ns$ models for $n=4, 6$, and 8 . The $\chi(T)$ curves are nearly identical to those obtained with the ns isolated chain models, that is, the effect of including $J(d3)$ on the computed $\chi(T)$ curves is negligible. Similar results were obtained when studying the effect of $J_{\text{ms}}^{\text{hq}}(d11)$ by using cyclic models (see Figure S3 in the Supporting Information). We also performed simulations of $\chi(T)$ by using a linear alternating chain minimal model of 12 magnetic centers that included the mediated through-space $J_{\text{ms}}^{\text{rad}}(d8)$ magnetic interaction of -0.31 cm^{-1} value (obtained with a trimer model, see Figure 5a for $J_{\text{ms}}^{\text{rad}}(d8)$ head-over-head (verdazyl-over-verdazyl) disposition). Once again, no difference was found (see Figure S4 in the Supporting Information).

All our findings indicated that the magnetism of the pyvd:hq co-crystal can be described by a set of almost independent 1D alternating chains, each of them containing two similar antiferromagnetic pair interactions. These interactions originate by means of the direct through-space interaction of adjacent pyridyl-verdazyl radicals packed in a head-over-tail relative orientation along the a axis. Our detailed analysis highlighted the need to look very carefully not just at crystal packing of radicals constituting the molecular magnet but, more importantly, at its magnetic topology. In this respect, although we could identify the magnetic pathways $d2$ and $d4$ as the dominant ones for the pyvd:hq co-crystal, we still cannot rationalize the specific origin of the relatively large exchange interaction in terms of any new magneto-structural correlation nor ascribe it to any atom-atom contact. This is due to the fact that the whole of the pyridyl-verdazyl radical is involved in the magnetic coupling process and not just the spin-carrying moiety of each pyridyl-verdazyl radical: both pyridyl and verdazyl rings are not isolated but electronically connected.

Conclusion

The application of a first-principles bottom-up procedure to the pyvd:hq crystal indicates the presence of two dominant antiferromagnetic interactions: $J(d2) = -54.43$ and $J(d4) = -55.97 \text{ cm}^{-1}$, computed at the UB3LYP/6-31+G(d) level. CASSCF(6,6) and CASSCF(10,10) calculations by using the same basis-set support the validity of these results. All other radical-radical magnetic interactions are computed to have values smaller than $|1.00| \text{ cm}^{-1}$.

The magnetic topology defined by these two interactions is a 1D alternating chain. The magnetic susceptibility is accurately reproduced, although it requires the use of a minimal chain model of larger length ($n=12$) than when regular chain models are used. The magnetic susceptibility curve is fully reproduced after applying a linear scaling factor of 1.17 to all the energies of the minimal chain model of 12 magnetic centers.

The $J(d2)$ and $J(d4)$ magnetic interactions are direct through-space interactions, which result from the direct overlap of the orbitals of the radicals. Contrarily to previous suggestions and the McConnell-I predictions, these head-over-tail magnetic interactions are not negligible. Our calculations show that, in all the cases evaluated in this crystal, the mediated through-space interactions are smaller than $|1.00| \text{ cm}^{-1}$ and, thus, should only be accounted for when no direct through-space interactions are present. CASCI calculations also indicate that they should be negligible in the pyvd:hq case. Therefore, we do not need to resort to mediated through-space interactions to explain the magnetism of the pyvd:hq molecular co-crystal.

Acknowledgements

M.D. and J.J.N. acknowledge the Spanish Ministerio de Ciencia y Tecnología (BQU2002-04587-C02-02), and the Catalan CIRIT (2001SGR-0044) for funding. The authors also thank the CEPBA-IBM Research Institute, CEPBA, and CESCA for allocation of CPU time on their computers. M.D. thanks the Spanish Ministerio de Educación y Ciencia for the award of a Ramón y Cajal Fellowship at Universitat de Barcelona. J.R.A. acknowledges the Spanish Ministerio de Educación y Ciencia for the award of his PhD grant.

- [1] a) *Magnetic Molecular Materials*, (Eds.: D. Gatteschi, O. Kahn, J. S. Miller, F. Palacio), NATO ASI Series, Kluwer, Dordrecht, **1991**; b) J. S. Miller, A. J. Epstein, *Angew. Chem.* **1994**, *106*, 399; *Angew. Chem. Int. Ed. Engl.* **1994**, *33*, 385; c) O. Kahn, *Molecular Magnetism*, VCH, New York, **1993**; d) *Molecular Magnetism: From Molecular Assemblies to the Devices* (Eds.: E. Coronado, P. Delhaès, D. Gatteschi, J. S. Miller), NATO ASI Series, Kluwer, Dordrecht, **1996**; e) *Magnetic Properties of Organic Materials* (Ed.: P. M. Lahti), Marcel Dekker, New York, **1999**; f) *Molecular Magnetism. New Magnetic Materials* (Eds.: K. Itoh, M. Kinoshita), Gordon and Breach, Amsterdam, **2000**; g) *π Electron Magnetism. From Molecules to Magnetic Materials* (Ed.: J. Veciana), *Structure and Bonding*, Vol. 100, Springer, **2001**; h) *Magnetism: Molecules to Materials (I-IV)* (Eds.: J. S. Miller, M. Drillon), Wiley-VCH, Weinheim, **2003**.
- [2] a) H. M. McConnell, *J. Chem. Phys.* **1963**, *39*, 1910; b) H. M. McConnell, *Proc. Robert A. Welch Found. Conf. Chem. Res.* **1967**,

- 11, 144; c) M. Deumal, J. J. Novoa, M. J. Bearpark, P. Celani, M. Olivucci, M. A. Robb, *J. Phys. Chem. A* **1998**, *102*, 8404; d) C. Kollmar, O. Kahn, *Acc. Chem. Res.* **1993**, *26*, 259.
- [3] R. Hicks, M. Lemaire, L. Öhrström, J. Richardson, L. Thompson, Xu Zhiqiang, *J. Am. Chem. Soc.* **2001**, *123*, 7154.
- [4] O. Kahn in *Molecular Magnetism*, VCH Publications, New York, **1993**, p. 252, Equation 11.1.5. Notice that this equation is based on $\hat{H}_{\text{fitting}} = -\sum J_{\text{fit}} \hat{S}_A \cdot \hat{S}_B$ to fit the experimental data. However, for all computational purposes, the Heisenberg Hamiltonian will be expressed as $\hat{H}_{\text{AB}} = -2\sum J_{\text{AB}} \hat{S}_A \cdot \hat{S}_B$. Therefore, when comparing J_{fit} to any computed J_{AB} , one must be aware that $J_{\text{fit}}/2 = J_{\text{AB}}$.
- [5] The difference between experimental (raw data) and fitted (by using $J_{\text{fit}} = -116 \text{ cm}^{-1}$ in Equation 11.1.5 from reference [4]) $\chi(T)$ values is almost constant ($\Delta\chi = 3 \times 10^{-4} \text{ emu mol}^{-1}$) and must be due to some uncorrected term (see Supporting Information Figure S1).
- [6] M. Deumal, M. J. Bearpark, J. J. Novoa, M. A. Robb, *J. Phys. Chem. A* **2002**, *106*, 1299.
- [7] a) M. Deumal, M. J. Bearpark, M. A. Robb, Y. Pontillon, J. J. Novoa, *Chem. Eur. J.* **2004**, *10*, 6422; b) M. Deumal, F. Mota, M. J. Bearpark, M. A. Robb, J. J. Novoa, *Mol. Phys.* **2006**, *104*, 857; c) M. Deumal, M. A. Robb, J. J. Novoa, *Polyhedron* **2003**, *22*, 1935; d) M. Deumal, M. A. Robb, J. J. Novoa, *Polyhedron* **2005**, *24*, 2368.
- [8] a) M. Deumal, G. Giorgi, M. A. Robb, M. M. Turnbull, C. P. Landee, J. J. Novoa, *Eur. J. Inorg. Chem.* **2005**, 4697; b) M. Deumal, C. P. Landee, J. J. Novoa, M. A. Robb, M. M. Turnbull, *Polyhedron* **2003**, *22*, 2235; c) M. Deumal, J. Ribas-Ariño, M. A. Robb, J. Ribas, J. J. Novoa, *Molecules* **2004**, *9*, 757.
- [9] Experimentally, susceptibility measurements are conducted at very low magnetic fields to avoid saturation effects in the magnetic data (e.g., by using a SQUID magnetometer). Thus, the expression for $\chi(T)$ has been derived at the zero-magnetic-field B limit. For more information, see: a) R. L. Carlin, *Magnetochemistry*, Springer, Heidelberg, **1986**; b) R. Boca, *Theoretical Foundations of Molecular Magnetism; Current Methods in Inorganic Chemistry, Vol. 1*, Elsevier Science S.A., The Netherlands, **1999**.
- [10] a) R. G. Parr, W. Yang, *Density-Functional Theory of Atoms and Molecules*, Oxford University Press, New York, **1989**; b) W. Koch, M. C. Holthausen, *A Chemist's Guide to Density Functional Theory*, 2nd ed, Wiley-VCH, Weinheim, **2000**.
- [11] a) L. Noodleman, *J. Chem. Phys.* **1981**, *74*, 5737; b) L. Noodleman, E. R. Davidson, *Chem. Phys.* **1986**, *109*, 131; c) E. Ruiz, P. Alemany, S. Alvarez, J. Cano, *J. Am. Chem. Soc.* **1997**, *119*, 1297; d) R. Caballol, O. Castell, F. Illas, I. D. R. Moreira, J. P. Malrieu, *J. Chem. Phys.* **1997**, *101*, 7860; e) M. Nishino, Y. Shigeta, T. Soda, Y. Kitagawa, T. Onishi, Y. Yoshioka, K. Yamaguchi, *Coord. Chem. Rev.* **2000**, *198*, 265; f) J.-M. Mouesca, *J. Chem. Phys.* **2000**, *113*, 10505; g) F. Illas, I. D. R. Moreira, C. de Graaf, V. Barone, *Theor. Chem. Acc.* **2000**, *104*, 265.
- [12] a) A. D. Becke, *Phys. Rev. A* **1988**, *38*, 3098; b) C. Lee, W. Yang, R. G. Parr, *Phys. Rev. B* **1988**, *37*, 785; c) A. D. Becke, *J. Chem. Phys.* **1993**, *98*, 5648.
- [13] 6-31+G(d) Basis set: R. Ditchfield, W. J. Hehre, J. A. Pople, *J. Chem. Phys.* **1971**, *54*, 724.
- [14] a) Gaussian 03 (Revision B.04), M. J. Frisch, G. W. Trucks, H. B. Schlegel, G. E. Scuseria, M. A. Robb, J. R. Cheeseman, J. A. Montgomery, Jr., T. Vreven, K. N. Kudin, J. C. Burant, J. M. Millam, S. S. Iyengar, J. Tomasi, V. Barone, B. Mennucci, M. Cossi, G. Scalmani, N. Rega, G. A. Petersson, H. Nakatsuji, M. Hada, M. Ehara, K. Toyota, R. Fukuda, J. Hasegawa, M. Ishida, T. Nakajima, Y. Honda, O. Kitao, H. Nakai, M. Klene, X. Li, J. E. Knox, H. P. Hratchian, J. B. Cross, C. Adamo, J. Jaramillo, R. Gomperts, R. E. Stratmann, O. Yazyev, A. J. Austin, R. Cammi, C. Pomelli, J. W. Ochterski, P. Y. Ayala, K. Morokuma, G. A. Voth, P. Salvador, J. J. Dannenberg, V. G. Zakrzewski, S. Dapprich, A. D. Daniels, M. C. Strain, O. Farkas, D. K. Malick, A. D. Rabuck, K. Raghavachari, J. B. Foresman, J. V. Ortiz, Q. Cui, A. G. Baboul, S. Clifford, J. Cioslowski, B. B. Stefanov, G. Liu, A. Liashenko, P. Piskorz, I. Komaromi, R. L. Martin, D. J. Fox, T. Keith, M. A. Al-Laham, C. Y. Peng, A. Nanayakkara, M. Challacombe, P. M. W. Gill, B. Johnson, W. Chen, M. W. Wong, C. Gonzalez, and J. A. Pople, Gaussian, Inc., Pittsburgh, PA, **2003**. b) GAMESS package: M. W. Schmidt, K. K. Baldridge, J. A. Boatz, S. T. Elbert, M. S. Gordon, J. H. Jensen, S. Koseki, N. Matsunaga, K. A. Nguyen, S. J. Su, T. L. Windus, M. Dupuis, J. A. Montgomery, *J. Comput. Chem.* **1993**, *14*, 1347.
- [15] Spin density evaluated at the UB3LYP/6-31+G(d) level using the GAUSSIAN package (ref. [14a]). Isodensity surface of 0.001 au.
- [16] See Figure 3b for $d10$ and $d11$ radical-radical geometries. The J_{AB} value of the $d11$ pair has been evaluated without including the hydroquinone molecule and was found to be $<|0.05| \text{ cm}^{-1}$. The J_{AB} value of $d10$ has also been evaluated including the hydroquinone molecule and was found to be numerically negligible.
- [17] E. Ruiz, A. Rodriguez-Forteza, J. Cano, S. Alvarez, P. Alemany, *J. Comput. Chem.* **2003**, *24*, 982.
- [18] For deficiencies of some functionals to describe magnetic systems: a) F. Illas, R. L. Martin, *J. Chem. Phys.* **1998**, *108*, 2519; b) C. de Graaf, C. Sousa, I. D. R. Moreira, F. Illas, *J. Phys. Chem. A*, **2001**, *105*, 11371; c) N. Queralt, C. de Graaf, J. Cabrero, R. Caballol, *Mol. Phys.* **2003**, *101*, 2095.
- [19] Strictly speaking, the term "charge-transfer" should only be used when the CASCI computation is done with orbitals of noninteracting monomers that are nonorthogonal.

Received: September 26, 2005
Published online: March 14, 2006